Electrochimica Acta, 1972, Vol. 17, pp. 861 to 871. Pergamon Press. Printed in Northern Ireland

POTENTIAL/pO^{2-} DIAGRAMS OF IRON, COBALT AND NICKEL IN MOLTEN SODIUM NITRITE*

S. L. MARCHIANO and A. J. ARVÍA
Instituto Superior de Investigaciones, División Electroquímica, Facultad de Ciencias Exactas, Universidad Nacional de La Plata, La Plata, Argentina

Abstract—Potential/pO^{2-} diagrams have been developed for iron, cobalt and nickel in molten sodium nitrite at 600 and 700°K. Four well defined regions corresponding respectively to metal corrosion, immunity, passivity and passivity breakdown are determined in the diagrams.

Résumé—On a développé les diagrammes potentiel/pO^{2-} pour les systèmes Fe(Co, Ni)/$NaNO_2$ fondue à des temperatures de 600 et 700°K. Ces diagrammes montrent quatre régions bien définies qui correspondent à la corrosion du métal, à l'immunité, à la passivité et à la rupture de la pellicule passive respectivement.

Zusammenfassung—Es wurden Potential/pO^{2-}-Diagramme für die Systeme Fe(Co, Ni)/geschmolzenes Natriumnitrit bei Temperaturen von 600 und 700°K aufgenommen. In diesen konnten vier gut definierte Bereiche bestimmt werden, die der Metallkorrosion, Immunität, Passivität, bzw. dem Zusammenbrechen der letzteren entsprechen.

INTRODUCTION

POTENTIAL/pO^{2-} diagrams constitute a useful presentation of thermodynamic data for establishing the direction of spontaneous reactions which the systems at equilibrium may undergo. In this way it is possible to envisage the regions of potential and oxide-ion activity where either immunity or corrosion or passivity of the metal occurs. Independently of the kinetics, an orientation about reaction products yielded by those processes can be obtained by means of the potential/pO^{2-} diagrams.

Thermodynamic diagrams were reported for various metals in molten chlorides.[1] Diagrams corresponding to silver, thallium, magnesium, nickel, cadmium, lead and iron in molten nitrates were also presented,[2,3] as well as a diagram for the iron/molten-sodium-sulphate system.[4] The equilibrium potentials of the possible decomposition reactions of various melts usually employed as electrolytes, such as carbonates, sulphates and nitrates have also been established.[5] For the latter, the thermodynamically favoured processes were determined.

The present paper reports the potential/pO^{2-} diagrams calculated for iron, cobalt and nickel electrodes in molten sodium nitrite, at 600 and 700°K. The occurrence of possible reaction products is also discussed.

CALCULATION PROCEDURE

The basis for calculating equilibrium potential/pO^{2-} diagrams is taken from the well known work of Pourbaix where equilibrium potential/pH diagrams for aqueous solutions of series of metals have been collected.[6] When Pourbaix' method is applied to a molten salt, the oxide-ion activity is taken as a measure of the basicity of the melt. This is a reasonable reference, as for oxyanion containing melts, the following equilibrium has been established[7]

$$XO_n^{z-} \rightleftarrows XO_{n-1}^{(z-2)-} + O^{2-} \qquad (1)$$

Therefore, the expression pO^{2-} in these melts is equivalent to the pH value in aqueous

* Manuscript received 16 April 1971.

solutions, and for nitrate and the nitrite melts, respectively, we have

$$NO_3^- \rightleftarrows NO_2^+ + O^{2-}, \tag{2}$$

and

$$NO_2^- \rightleftarrows NO^+ + O^{2-}. \tag{3}$$

To calculate the potential of the different half-reactions, the nitrate electrode at $p_{NO_2} = p_{O_2} = 1$ atm has been chosen as reference ($E^\circ = 0$). The electrode equilibrium is represented as

$$2\,NO_2(g, p = 1) + O_2(g, p = 1) + 2\,e = 2\,NO_3^-(l). \tag{4}$$

The standard free energy change of reaction (4) is consequently taken as zero ($\Delta G_4^\circ = 0$).

The standard free energy change ΔG_T° at temperature T of any equilibrium can be obtained from

$$\Delta G_T^\circ = \Delta H_T^\circ - T\Delta S_T^\circ, \tag{I}$$

where ΔH_T° and ΔS_T° are respectively the enthalpy and entropy differences between the corresponding products and reactants, at T°K. The latter values are obtained from different compilations of thermodynamic data.[8–10] From the ΔG_T° value, the standard electrode potential of the equilibrium is

$$E^\circ = -zF\Delta G_T^\circ. \tag{II}$$

After the E° value has been obtained the corresponding Nernst expression is immediately given. When no thermal data for a particular compound are available, a calculation of its thermodynamic quantities is approximated either with the aid of known data of structurally related species or by means of the Born–Haber cycle and Hess' law.

Possible reactions related to sodium nitrite decomposition

From the thermodynamic viewpoint, the nitrite ion can participate in various electrode equilibria involving N_2, N_2O, NO, NO_2, O^{2-} and O_2, according to the following reactions,

$$NO_2(g) + e \rightleftarrows NO_2^-(l), \tag{5}$$

$$2\,NO_2^-(l) + 6\,e \rightleftarrows N_2(g) + 4\,O^{2-}(l), \tag{6}$$

$$2\,NO_2^-(l) + 4\,e \rightleftarrows N_2O(g) + 3\,O^{2-}(l), \tag{7}$$

$$NO_2^-(l) + e \rightleftarrows NO(g) + O^{2-}(l), \tag{8}$$

$$NO_2(g) + NO_2^-(l) + e \rightleftarrows 2\,NO(g) + \tfrac{1}{2}\,O_2(g) + O^{2-}(l). \tag{9}$$

Reactions (6) to (9) depend on the oxide-ion activity. Apart from these reactions, nitrite ion may be formed either according to

$$NO(g) + \tfrac{1}{2}\,O_2(g) + e \rightleftarrows NO_2^-(l), \tag{10}$$

or from nitrate ion, if the latter is present, as follows,

$$NO_3^-(l) + 2\,e \rightleftarrows NO_2^-(l) + O^{2-}(l). \tag{11}$$

Furthermore, the presence of oxide ion and oxygen gas together imply the existence

of the oxygen-electrode reaction in the melt,

$$\tfrac{1}{2}\,O_2(g) + 2\,e \rightleftarrows O^{2-}(l) \qquad (12)$$

and, similarly, the existence of NO_2 suggests the equilibrium

$$NO_2(g) + 2\,e \rightleftarrows NO(g) + O^{2-}(l). \qquad (13)$$

The E° values and the Nernst equations of reactions (5) to (13) are assembled in Table 1, at 600 and 700°K. The dependence of the electrode potentials on pO^{2-} for the different reactions is shown in Figs. 1 and 2.

TABLE 1

Equilibrium	ΔG°_{600} kcal/mol	E°_{600} V	ΔG°_{700} kcal/mol	E°_{700} V
$2\,NO_3(p=1) + O_2(p=1) + 2\,e \rightleftarrows 2\,NO_3^-(l)$	0	0	0	0
$E = E^\circ + \frac{2{\cdot}303RT}{2F}\log\frac{(p_{NO_3})^2(p_{O_2})}{(a_{NO_3^-})^2}$				
$NO_3^-(l) + e \rightleftarrows NO(g) + O^{2-}(l)$	65·33	−2·832	55·45	−2·4
$E = E^\circ + \frac{2{\cdot}303RT}{F}\log\frac{(a_{NO_3^-})}{(p_{NO})} + \frac{2{\cdot}303RT}{F}pO^{2-}$				
$NO_3^-(l) + NO_2(g) + e \rightleftarrows 2\,NO(g) + \frac{1}{2}\,O_2(g) + O^{2-}(l)$	68·27	−2·960	56·57	−2·453
$E = E^\circ + \frac{2{\cdot}303RT}{F}\log\frac{(p_{NO_2})(a_{NO_3^-})}{(p_{NO})^2(p_{O_2})^{1/2}} + \frac{2{\cdot}303RT}{F}pO^{2-}$				
$2\,NO_3^-(l) + 4\,e \rightleftarrows N_2O(g) + 3\,O^{2-}(l)$	202·27	−2·192	179.93	−1.950
$E = E^\circ + \frac{2{\cdot}303RT}{4F}\log\frac{(a_{NO_3^-})^2}{(p_{N_2O})} + \frac{3(2{\cdot}303RT)}{4F}pO^{2-}$				
$2\,NO_3^-(l) + 6\,e \rightleftarrows N_2(g) + 4\,O^{2-}(l)$	253·18	−1·829	221·86	−1·603
$E = E^\circ + \frac{2{\cdot}303RT}{6F}\log\frac{(a_{NO_3^-})^2}{(p_{N_2})} + \frac{4(2{\cdot}303RT)}{6F}pO^{2-}$				
$NO_2(g) + e \rightleftarrows NO_2^-(l)$	18·69	−0·810	18·43	−0·799
$E = E^\circ + \frac{2{\cdot}303RT}{F}\log\frac{(p_{NO_2})}{(a_{NO_2^-})}$				
$NO_2(g) + 2\,e \rightleftarrows NO(g) + O^{2-}(l)$	84·02	−1·821	74·99	−1·626
$E = E^\circ + \frac{2{\cdot}303RT}{2F}\log\frac{(p_{NO_2})}{(p_{NO})} + \frac{2{\cdot}303RT}{2F}pO^{2-}$				
$NO(g) + \frac{1}{2}\,O_2(g) + e \rightleftarrows NO_2^-(l)$	15·75	−0·683	17·30	−0·750
$E = E^\circ + \frac{2{\cdot}303RT}{F}\log\frac{(a_{NO_2^-})}{(p_{NO})(p_{O_2})^{1/2}}$				
$NO_3^-(l) + 2\,e \rightleftarrows NO_2^-(l) + O^{2-}(l)$	99·77	−2·163	92·30	−2.001
$E = E^\circ + \frac{2{\cdot}303RT}{2F}\log\frac{(a_{NO_3^-})}{(a_{NO_2^-})} + \frac{2{\cdot}303RT}{2F}pO^{2-}$				
$\frac{1}{2}\,O_2(g) + 2\,e \rightleftarrows O^{2-}$	81·08	−1·758	73·87	−1·601
$E = E^\circ + \frac{2{\cdot}303RT}{2F}\log(p_{O_2})^{1/2} + \frac{2{\cdot}303RT}{2F}pO^{2-}$				

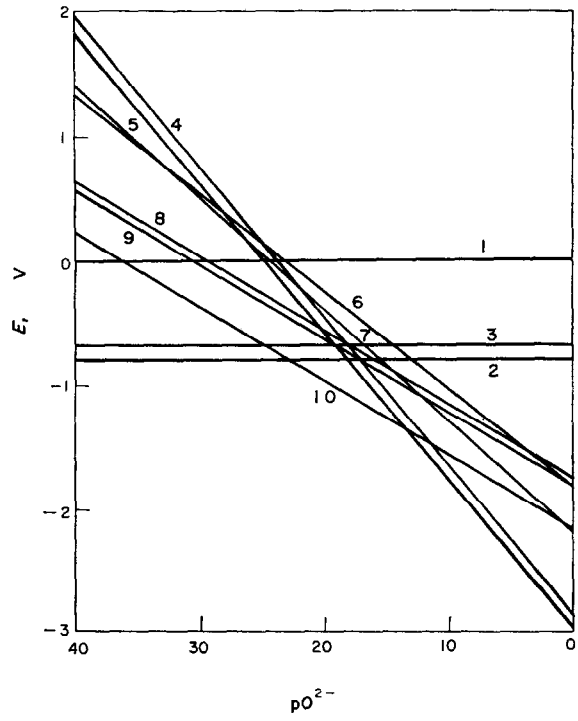

FIG. 1. Potential/pO^{2-} diagram for reactions involving the nitrite ion and related compounds at 600°K.

1. Reference reaction
   $2\,NO_2(g, p = 1) + O_2(g, p = 1) + 2\,e \rightleftarrows 2\,NO_2^-(l)$.
2. $NO_2(g) + e = NO_2^-(l)$.
3. $NO(g) + \frac{1}{2}\,O_2(g) + e = NO_2^-(l)$.
4. $NO_2^-(l) + e = NO(g) + O^{2-}(l)$.
5. $NO_2(g) + NO_2^-(l) + e = 2\,NO(g) + \frac{1}{2}\,O_2(g) + O^{2-}(l)$.
6. $2\,NO_2^-(l) + 6\,e = N_2(g) + 4\,O^{2-}(l)$.
7. $2\,NO_2^-(l) + 4\,e = N_2O(g) + 3\,O^{2-}(l)$.
8. $\frac{1}{2}\,O_2(g) + 2\,e = O^{2-}(l)$.
9. $NO_2(g) + 2\,e = NO(g) + O^{2-}(l)$.
10. $NO_3^-(l) + 2\,e = NO_2^-(l) + O^{2-}(l)$.

The potential/pO^{2-} diagram for the molten sodium nitrite reveals, from a thermodynamic viewpoint and for unitary activity of products and reactants except the oxide-ion activity, that nitrite ion decomposition according to (10) is favoured at low pO^{2-} values, whereas at high pO^{2-} values, equilibrium (6) is the energetically preferred over-all process. These conclusions, however, as far as rate processes are concerned, should be taken cautiously because of the more or less marked irreversibility of any of the electron-transfer processes shown in the diagram. Furthermore, electrochemical kinetics indicates that any multiple electron-transfer over-all reaction quite likely involves a mechanism where charge-transfer steps occur with the transfer of one electron. This fact puts a limit to the derivation of kinetic and mechanistic conclusions from the potential/pO^{2-} diagrams.

POTENTIAL/pO^{2-} DIAGRAM FOR IRON

Once the equilibrium diagram for sodium nitrite is established the equilibria involving iron, iron ions, oxide ion and the different iron oxides can be considered.

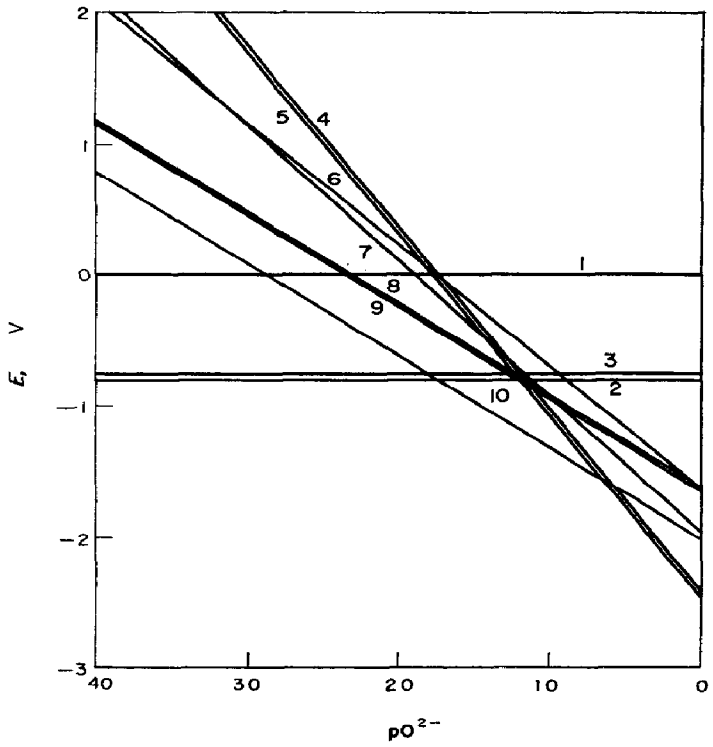

FIG. 2. Potential/pO^{2-} diagram for reactions involving the nitrite ion and related compounds at 700°K. The numbers correspond to the equilibria indicated in Fig. 1.

As these equilibria have already been calculated for the potential/pO^{2-} diagram for iron in molten sodium nitrate at 600 and 700°K, they are taken from the previous publication.[3] Figs. 3 and 4 show the potential/pO^{2-} diagram at 600 and 700°K respectively for iron.

POTENTIAL/pO^{2-} DIAGRAM FOR COBALT

Following the calculation procedure indicated above the same considerations are applied to calculate the potential/pO^{2-} diagram for cobalt. Co^{2+} ion exists as a stable entity at low temperature and at the temperatures of the present calculation. Co^{3+} ion apparently occurs at low temperature in aqueous solutions, but it reduces to Co^{2+} with the oxidation of water. No data are reported for the Co^{3+} ion at high temperature. There are thermodynamic data of the CoO and Co_3O_4 oxides, but no data were found for Co_2O_3. At room temperature the existence of of CoO_2 has been reported. However, this compound is very unstable, at least in the presence of water. No data exist for this oxide at high temperature. It is likely that the compound is also unstable in the molten media. Consequently only the following equilibria have been considered for the case of cobalt,

$$CoO(s) + 2\,e \rightleftarrows Co(s) + O_2^-(l), \quad (14)$$

$$Co_3O_4(s) + 2\,e \rightleftarrows 3CoO(s) + O^{2-}(l), \quad (15)$$

$$Co^{2+}(l) + 2\,e \rightleftarrows Co(s), \quad (16)$$

$$CoO(s) \rightleftarrows Co^{2+}(l) + O^{2-}(l), \quad (17)$$

$$Co_3O_4(s) + 2\,e \rightleftarrows 3\,Co^{2+}(l) + 4\,O^{2-}(l). \quad (18)$$

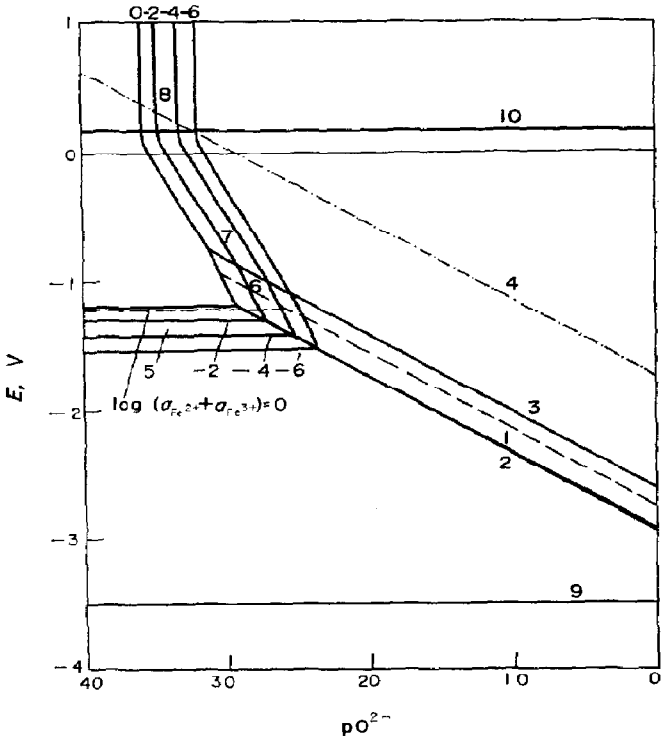

FIG. 3. Potential/pO^{2-} diagram for iron electrode and iron-oxide reactions at 600°K.

1. $Fe_3O_4(s) + 2\,e = 3\,FeO(s) + O^{2-}(l)$.
2. $FeO(s) + 2\,e = Fe(s) + O^{2-}(l)$.
3. $3\,Fe_2O_3(s) + 2\,e = 2\,Fe_3O_4(s) + O^{2-}(l)$.
4. $\frac{1}{2}\,O_2(g) + 2\,e = O^{2-}(l)$.
5. $Fe^{2+}(l) + 2\,e = Fe(s)$.
6. $Fe_3O_4(s) + 2\,e = 3\,Fe^{2+} + 4\,O^{2-}(l)$.
7. $Fe_2O_3(s) + 2\,e = 2\,Fe^{3+}(l) + 3\,O^{2-}(l)$.
8. $Fe_2O_3(s) = 2\,Fe^{3+}(l) + 3\,O^{2-}(l)$.
9. $Na^{+}(l) + e = Na(l)$.
10. $Fe^{3+}(l) + e = Fe^{2+}(l)$.

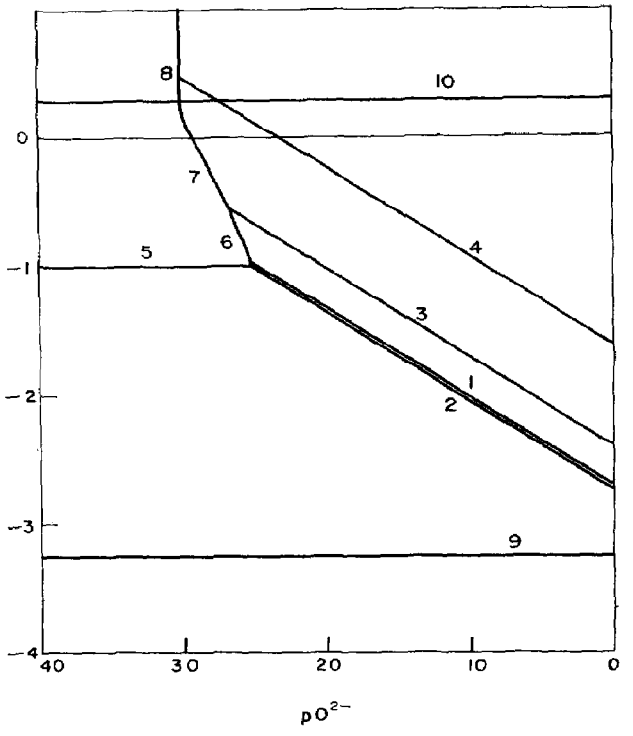

FIG. 4. Potential/pO^{2-} diagram for iron electrode and iron-oxide reactions at 700°K. The numbers correspond to the equilibria indicated in Fig. 3.

Thermal data for reactions (14) to (18) are available and allow the calculation of E° and Nernst equations, as compiled in Table 2. The dependence of the electrode potentials on pO^{2-} is illustrated in Figs. 5 and 6, for 600 and 700°K.

TABLE 2

Equilibrium	ΔG°_{600} kcal/mol	E°_{600} V	ΔG°_{700} kcal/mol	E°_{700} V
$Co^{2+}(l) + 2\,e \rightleftarrows Co(s)$	49·20	−1·067	39·98	−0·867
$E = E^\circ + \frac{2{\cdot}303RT}{2F} \log (a_{Co^{2+}})$				
$CoO(s) + 2\,e \rightleftarrows Co(s) + O^{2-}(l)$	126·14	−2·734	117·36	−2·540
$E = E^\circ + \frac{2{\cdot}303RT}{2F} pO^{2-}$				
$Co_3O_4(s) + 2\,e \rightleftarrows 3\,CoO(s) + O^{2-}(l)$	104·39	−2·263	93·96	−2·036
$E = E^\circ + \frac{2{\cdot}303RT}{2F} pO^{2-}$				
$Co_3O_4(s) + 2\,e \rightleftarrows 3\,Co^{2+}(l) + 4\,O^{2-}(l)$	335·39	−7·270	325·16	−7·049
$E = E^\circ + \frac{2{\cdot}303RT}{2F} \log (a_{Co^{2+}})^3 + \frac{4(2{\cdot}303RT)}{2F} pO^{2-}$				

POTENTIAL/pO^{2-} DIAGRAM FOR NICKEL

For nickel, as far as the possibility of oxygen compounds participating in corrosion and passivation phenomena is concerned, the situation is even more restricted than in the case of cobalt and iron, since no thermal data of any nickel oxide higher than NiO have been published to the authors' knowledge. This fact is undoubtedly related to the failure of its preparation and identification of higher nickel oxides.[11] The existence of nickel oxides as stoichiometric compounds higher than NiO having proper lattice constants is not yet definitely established. However, various publications are devoted to calculating thermodynamic data of different stoichiometry, where structural similarities between nickel oxide and magnesium oxide were taken for the caculations.[12] Some authors assume that oxygen atoms adsorb on the NiO surface, and after migration to the inner matrix, stabilize within the crystal in a vacancy site. The uncertainty about higher nickel oxides does not allow us to consider them in the Ni/pO^{2-} diagram except for NiO. Therefore, the equilibria considered are

$$Ni^{2+}(l) + 2\,e \rightleftarrows Ni(s), \tag{19}$$

$$NiO(s) + 2\,e \rightleftarrows Ni(s) + O^{2-}(l), \tag{20}$$

$$NiO(s) \rightleftarrows Ni^{2+}(l) + O^{2-}(l). \tag{21}$$

The E° values and Nernst equations calculated for these reactions are assembled in Table 3 and the dependence of the potentials on the oxide ion activity is illustrated in Fig. 7 for 500°K and in Fig. 8 for 600 and 700°K.

CHARACTERISTIC FEATURES OF THE E/pO^{2-} DIAGRAMS FOR Fe, Co AND Ni IN MOLTEN $NaNO_2$

Although the three E/pO^{2-} diagrams comprise different patterns they present some common features that can be analysed simultaneously for the three metals. There is a region of immunity where the metallic state is stable. The limits of this

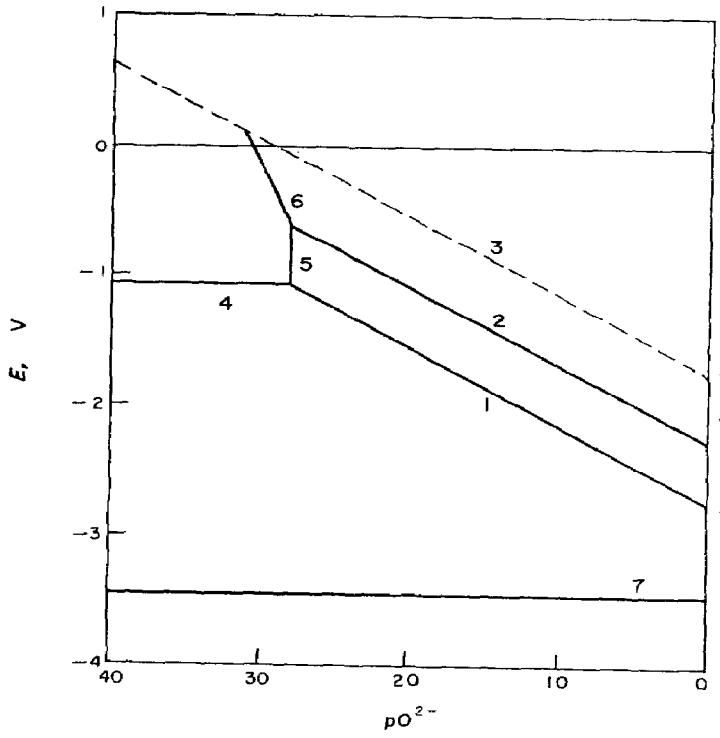

FIG. 5. Potential/pO^{2-} diagram for the cobalt electrode and cobalt oxides redox reactions at 600°K.

1. $CoO(s) + 2\,e \rightleftharpoons Co(s) + O^{2-}(l)$.
2. $Co_3O_4(s) + 2\,e = 3\,CoO(s) + O^{2-}(l)$.
3. $\frac{1}{2}\,O_2(g) + 2\,e = O^{2-}(l)$.
4. $Co^{2+}(l) + 2\,e = Co(s)$.
5. $CoO(s) = Co^{2+}(l) + O^{2-}(l)$.
6. $Co_3O_4(s) + 2\,e = 3\,Co^{2+}(l) + 4\,O^{2-}(l)$.
7. $Na^{+}(l) + e = Na(l)$.

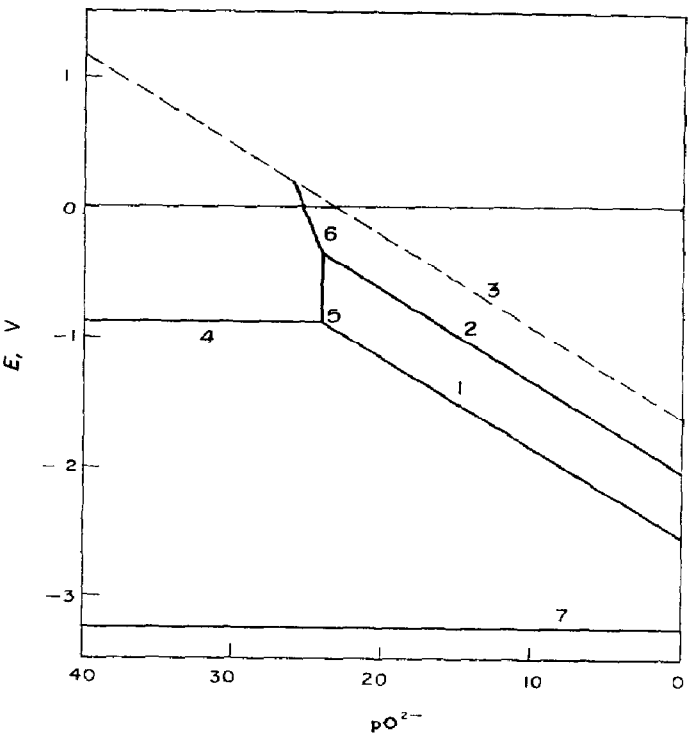

FIG. 6. Potential/pO^{2-} diagram for the cobalt electrode and cobalt oxides redox reactions at 700°K. Numbers correspond to the equilibria indicated in Fig. 5.

TABLE 3

Equilibrium	ΔG°_{600} kcal/mol	E°_{600} V	ΔG°_{700} kcal/mol	E°_{700} V
$Ni^{2+}(l) + 2e = Ni(s)$	46·47	−1·007	36·94	−0·801
$E = E^\circ + \frac{2{\cdot}303RT}{2F} \log (a_{Ni^{2+}})$				
$NiO(s) + 2e = Ni(s) + O^{2-}(l)$	126·21	−2·736	116·89	−2·534
$E = E^\circ + \frac{2{\cdot}303RT}{2F} pO^{2-}$				

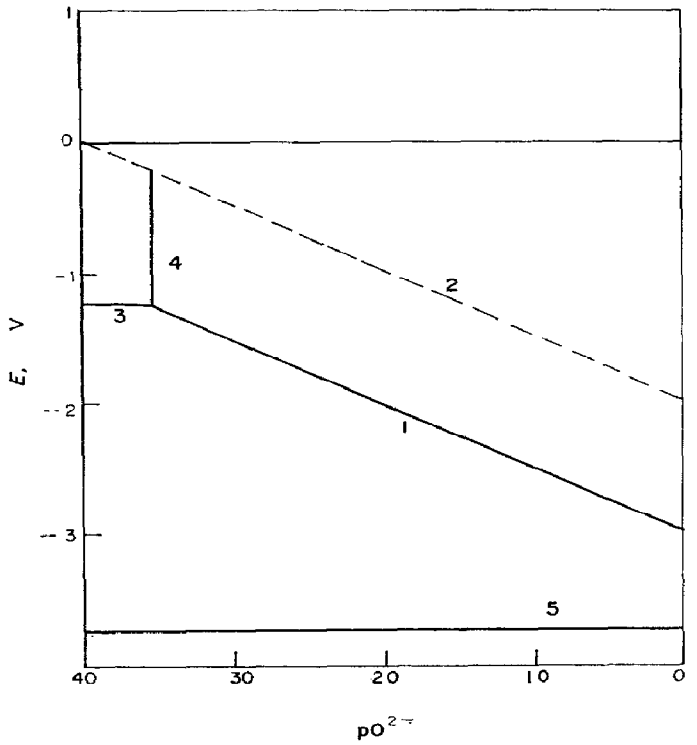

FIG. 7. Potential/pO^{2-} diagram for nickel electrode and nickel oxide redox reactions at 500°K.
1. $NiO(s) + 2e \rightleftarrows Ni(s) + O^{2-}(l)$.
2. $\frac{1}{2} O_2(g) + 2e = O^{2-}(l)$.
3. $Ni^{2+}(l) + 2e = Ni(s)$.
4. $NiO(s) = Ni^{2+}(l) + O^{2-}(l)$.
5. $Me^{+}(l) + e = Me(l)$.
Me = K.

region are the lines defining the metal/metal-oxide and metal/ionic-dissolved-metal equilibria, depending on the activity of oxide ions in the melt. A second region is distinguished at higher anodic potentials and low oxide-ion activity, where the stable species is the metal ion dissolved in the molten salt. This area is limited by equilibria comprising oxide or metal/ionic species. The number of these equilibria that may participate in the corrosion and passivation phenomena depends on the metal. Thus, three equilibria could be calculated for iron, two for cobalt and only one for nickel.

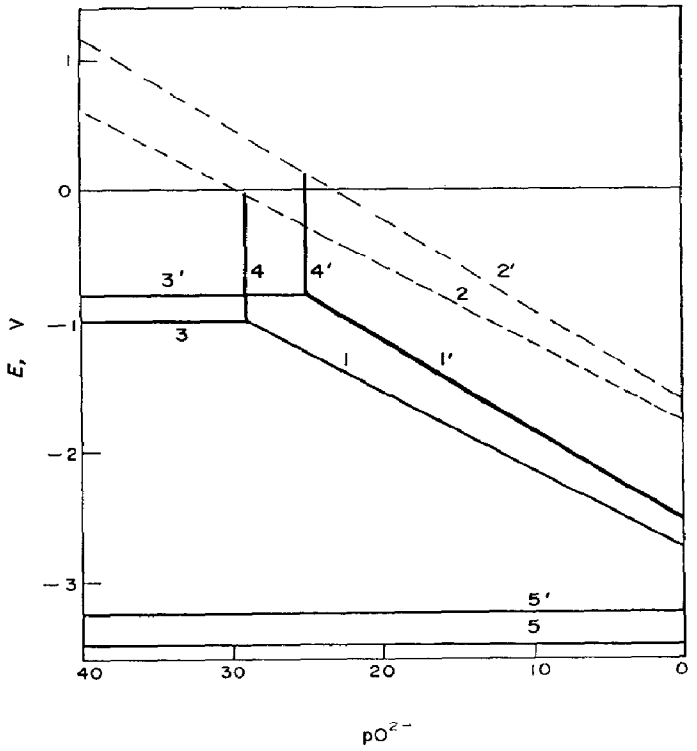

FIG. 8. Potential/pO^{2-} diagram for nickel electrode and nickel oxide redox reactions at 600 and 700°K. Numbers correspond to the equilibria indicated in Fig. 7. Me = Na. Dashed numbers refer to 700°K.

The number on metal/oxide equilibria appears directly related to the atomic structure of the metal. The third region corresponds to passivity and it extends at potentials above the metal/metal-oxide equilibrium line and toward the region of higher oxide-ion activity. This region is limited at high anodic potentials by the reversible oxygen-electrode line. In this region the various metal-oxide(I)/metal-oxide(II) equilibria are comprised. For the case of iron the lines of the three equilibria are

$$Fe_3O_4(s) + 2\,e \rightleftarrows 3\,FeO(s) + O^{2-}(l), \tag{22}$$

$$FeO(s) + 2\,e \rightleftarrows Fe(s) + O^{2-}(l), \tag{23}$$

and

$$Fe_2O_3(s) + 2\,e \rightleftarrows 2\,Fe_3O_4(s) + O^{2-}(l). \tag{24}$$

are relatively close. The two former equilibria, however, comprise a zone of thermodynamic instability. As a matter of fact, the thermodynamic calculation with tabulated data indicates that iron undergoes oxidation to magnetite at a potential lower than that corresponding to its oxidation to ferrous oxide. This result implies the occurrence of the equilibrium

$$Fe_3O_4(s) + Fe(s) \rightleftarrows 4\,FeO(s). \tag{25}$$

However, this effect is not observed at 700°K, as the lines corresponding to the different equilibria are located in the order expected according to the degree of oxidation of the metal. The presence of the various iron oxides has been proved by

X-ray diffractometry.[13] These facts are reflected in the anodic behaviour of the iron electrodes in molten sodium nitrate,[14] after considering the possible departure of kinetic experiments from the equilibrium conditions predicted by the E/pO^{2-} diagram.

The passive region for the cobalt electrode comprises only two oxides species and the equilibria

$$CoO(s) + 2\,e = Co(s) + O^{2-}(l) \tag{26}$$

and

$$Co_3O_4(s) + 2\,e = 3\,CoO(s) + O^{2-}(l). \tag{27}$$

The standard free energy of these reactions are rather separated, the value corresponding to reaction (27) approaching the standard free energy of the oxygen-electrode reaction.

Finally, in the case of nickel only one oxide equilibrium can be calculated,

$$NiO(s) + 2\,e = Ni(s) + O^{2-}(l) \tag{28}$$

and apparently in the potential region extending up to the oxygen-electrode reaction no other equilibrium exists involving any nickel oxide species with a higher degree of oxidation.

By coupling together the E/pO^{2-} diagram of the molten nitrite with those of the metals, interesting information can be obtained about the possible existence of mixed potentials and the probable reactions comprised there. Precisely, these diagrams are useful to correlate kinetic information of the iron and nickel electrodes in molten alkali nitrites[15] and they are being applied for the case of cobalt, as will be reported in the near future.

Acknowledgement—The authors thank the Consejo Nacional de Investigaciones Científicas y Técnicas of Argentina for partial financial support. S. L. M. acted as a Faculty Member of the Departmento de Ingeniería Química de la Facultad de Ingeniería de la Universidad Nacional de La Plata.

REFERENCES

1. R. Littlewood, *J. electrochem. Soc.* **109,** 525 (1962).
2. A. Conte and S. Casadio, *Ric. Sci.* **36,** 3 (1966).
3. S. L. Marchiano and A. J. Arvía, *Electrochim. Acta* **17,** 25 (1972).
4. G. Baudo and A. Tamba, *Brit. Corros. J.* **4,** 130 (1969).
5. H. E. Bartlett and K. E. Johnson, *Can. J. Chem.* **44,** 2119 (1966).
6. M. Pourbaix, *Atlas of Electrochemical Equilibria in Aqueous Solutions*. Pergamon, Oxford (1966).
7. R. N. Kunst and F. R. Duke, *J. Am. chem. Soc.* **85,** 3338 (1963).
8. K. K. Kelly, *Contribution to the Data in Theoretical Metallurgy, XIII, High Temperature, Heat Content, Heat Capacity and Entropy Data for the Elements and Inorganic Compounds.* Bull. 5841, Bureau of Mines, U.S.A. (1960).
9. *Selected Values of Chemical Thermodynamic Properties*, National Bureau of Standards, Circular 500, U.S.A. (1952).
10. O. Kubaschevski and E. L. Evans, *Metallurgical Thermochemistry*. Pergamon, London (1958).
11. J. Labat, *J. Chim. phys.* **60,** 1251 (1963).
12. D. Mehandjiev, *C. r. Acad. bulg. Sci.* **22,** 1253 (1969).
13. R. G. Casino, J. J. Podestá and A. J. Arvía, *Electrochim. Acta* **16,** 121 (1971).
14. A. J. Arvía, J. J. Podestá and R. C. V. Piatti, *Electrochim. Acta* **17,** 25 (1972).
15. A. J. Arvía, R. C. V. Piatti and J. J. Podestá, *Electrochim. Acta* **17,** 889 (1972).